



# Advancing research:

*One cell at a time*

*One scientist at a time*

*One discovery at a time*

**Proven solutions  
that further science**

BD Accuri™ C6 Plus

BD FACSCelesta™

BD LSRFortessa™

**Discover more >**



[www.bdbiosciences.com/us/go/research-solutions](http://www.bdbiosciences.com/us/go/research-solutions)



# Heat shock protein 70 and tumor-infiltrating NK cells as prognostic indicators for patients with squamous cell carcinoma of the head and neck after radiochemotherapy: A multicentre retrospective study of the German Cancer Consortium Radiation Oncology Group (DKTK-ROG)

Stefan Stangl<sup>1,2,3</sup>, Nikoleta Tontcheva<sup>4</sup>, Wolfgang Sievert<sup>1,2,3</sup>, Maxim Shevtsov<sup>1,2,3</sup>, Minli Niu<sup>1</sup>, Thomas E. Schmid<sup>1,2,3</sup>, Steffi Pigorsch<sup>1,2,3</sup>, Stephanie E. Combs<sup>1,2,3</sup>, Bernhard Haller<sup>5</sup>, Panagiotis Balermipas<sup>6,7</sup>, Franz Rödel<sup>6,7</sup>, Claus Rödel<sup>6,7</sup>, Emmanouil Fokas<sup>6,7</sup>, Mechthild Krause<sup>8,9,10,11</sup>, Annett Linge<sup>8,9,10</sup>, Fabian Lohaus<sup>8,9,10</sup>, Michael Baumann<sup>8,9,10,12</sup>, Inge Tinhofer<sup>13,14</sup>, Volker Budach<sup>13,14</sup>, Martin Stuschke<sup>15,16</sup>, Anca-Ligia Grosu<sup>17,18</sup>, Amir Abdollahi<sup>12</sup>, Jürgen Debus<sup>12,19,20</sup>, Claus Belka<sup>3,20,21,22</sup>, Cornelius Maihöfer<sup>3,20,21,22</sup>, David Mönnich<sup>23,24,25</sup>, Daniel Zips<sup>23,24,25</sup> and Gabriele Multhoff<sup>1,2,3</sup>

<sup>1</sup> Department of Radiation Oncology, Klinikum rechts der Isar, Technische Universität München (TUM), Munich, Germany

<sup>2</sup> Department of Radiation Sciences (DRS), Helmholtz Zentrum Munich (HMGU), Institute of Innovative Radiotherapy (iRT), Munich, Germany

<sup>3</sup> German Cancer Research Centre (DKFZ), Heidelberg and German Research Consortium (DKTK), Munich, Germany

<sup>4</sup> MVZ Radiologie und Strahlentherapie Nürnberg, Nürnberg, Germany

<sup>5</sup> Institute of Medical Informatics, Statistics and Epidemiology, Technische Universität München (TUM), Munich, Germany

<sup>6</sup> Department of Radiotherapy and Oncology, Goethe University Frankfurt, Germany

<sup>7</sup> German Cancer Research Centre (DKFZ), Heidelberg and German Research Consortium (DKTK), Frankfurt, Frankfurt, Germany

<sup>8</sup> OncoRay – National Centre for Radiation Research in Oncology, Faculty of Medicine and University Hospital Carl Gustav Carus, Technische Universität Dresden, Dresden, Germany

<sup>9</sup> Department of Radiation Oncology, Faculty of Medicine and University Hospital Carl Gustav Carus, Technische Universität Dresden, Dresden, Germany

<sup>10</sup> German Cancer Research Centre (DKFZ), Heidelberg and German Research Consortium (DKTK), Dresden, Germany

<sup>11</sup> Helmholtz-Zentrum Dresden – Rossendorf, Institute of Radiooncology, Berlin, Germany

<sup>12</sup> German Cancer Research Centre (DKFZ), Heidelberg and German Research Consortium (DKTK), Heidelberg, Germany

<sup>13</sup> Department of Radiooncology and Radiotherapy, Charite University Hospital Berlin, Berlin, Germany

<sup>14</sup> German Cancer Research Centre (DKFZ), Heidelberg and German Research Consortium (DKTK), Berlin, Germany

<sup>15</sup> Department of Radiotherapy, Medical Faculty, University of Duisburg-Essen, Essen, Germany

<sup>16</sup> German Cancer Research Centre (DKFZ), Heidelberg and German Research Consortium (DKTK), Essen, Germany

<sup>17</sup> Department of Radiation Oncology, Medical Faculty, Medical Centre, University of Freiburg, Germany

<sup>18</sup> German Cancer Research Centre (DKFZ), Heidelberg and German Research Consortium (DKTK), Freiburg, Germany

<sup>19</sup> Department of Radiation Oncology, Heidelberg Ion Therapy Centre (HIT), Heidelberg Institute of Radiation Oncology (HIRO), University of Heidelberg Medical School, Heidelberg, Germany

<sup>20</sup> National Centre for Radiation Research Oncology (NCRO), University of Heidelberg Medical School, Heidelberg, Germany

<sup>21</sup> Department of Radiation Oncology, University Hospital LMU Munich, Munich, Germany

<sup>22</sup> Clinical Cooperation Group (CCG) Personalized Radiotherapy in Head and Neck Cancer, Helmholtz Zentrum, Munich, Germany

<sup>23</sup> Department of Radiation Oncology, Faculty of Medicine and University Hospital Tübingen, Eberhard Karls University Tübingen, Tübingen, Germany

<sup>24</sup> DKTK Consortium Tübingen, Tübingen, Germany

<sup>25</sup> German Cancer Research Centre (DKFZ), Heidelberg and German Research Consortium (DKTK), Tübingen, Germany

**Key words:** Hsp70, prognostic biomarker, SCCHN, NK cells, IHC, retrospective trial

**Grant sponsor:** Bundesministerium für Bildung und Forschung; **Grant numbers:** 02NIK038A, 01GU0823; **Grant sponsor:** EU CELLEUROPE; **Grant number:** EU 315963; **Grant sponsor:** Deutsche Forschungsgemeinschaft; **Grant numbers:** SFB824/3, STA1520/1-1; **Grant sponsor:** Federal Ministry for Economic Affairs and Energy; **Grant number:** ZF4320102CS7; **Grant sponsor:** DFG and the Technische Universität München within the funding programme Open Access Publishing

**DOI:** 10.1002/ijc.31213

This is an open access article under the terms of the Creative Commons Attribution-NonCommercial License, which permits use, distribution and reproduction in any medium, provided the original work is properly cited and is not used for commercial purposes.

**History:** Received 11 Sep 2017; Accepted 28 Nov 2017; Online 13 Dec 2017

**Correspondence to:** Gabriele Multhoff, Department of Radiation Oncology, Klinikum rechts der Isar, TU München (TUM), Ismaninger Str. 22, 81675 Munich, Germany, E-mail: gabriele.multhoff@tum.de; Tel: +49 8941404514

Tumor cells frequently overexpress heat shock protein 70 (Hsp70) and present it on their cell surface, where it can be recognized by pre-activated NK cells. In our retrospective study the expression of Hsp70 was determined in relation to tumor-infiltrating CD56<sup>+</sup> NK cells in formalin-fixed paraffin embedded (FFPE) tumor specimens of patients with SCCHN ( $N = 145$ ) as potential indicators for survival and disease recurrence. All patients received radical surgery and postoperative cisplatin-based radiochemotherapy (RCT). In general, Hsp70 expression was stronger, but with variable intensities, in tumor compared to normal tissues. Patients with high Hsp70 expressing tumors (scores 3–4) showed significantly decreased overall survival (OS;  $p = 0.008$ ), local progression-free survival (LPFS;  $p = 0.034$ ) and distant metastases-free survival (DMFS;  $p = 0.044$ ), compared to those with low Hsp70 expression (scores 0–2), which remained significant after adjustment for relevant prognostic variables. The adverse prognostic value of a high Hsp70 expression for OS was also observed in patient cohorts with p16- ( $p = 0.001$ ), p53- ( $p = 0.0003$ ) and HPV16 DNA-negative ( $p = 0.001$ ) tumors. The absence or low numbers of tumor-infiltrating CD56<sup>+</sup> NK cells also correlated with significantly decreased OS ( $p = 0.0001$ ), LPFS ( $p = 0.0009$ ) and DMFS ( $p = 0.0001$ ). A high Hsp70 expression and low numbers of tumor-infiltrating NK cells have the highest negative predictive value ( $p = 0.0004$ ). In summary, a strong Hsp70 expression and low numbers of tumor-infiltrating NK cells correlate with unfavorable outcome following surgery and RCT in patients with SCCHN, and thus serve as negative prognostic markers.

#### What's new?

It's difficult to predict how a patient with squamous-cell carcinoma of the head and neck (SCCHN) will respond to treatment, because every tumor is different. In this study, the authors identified two pre-treatment measures that were associated with poor prognosis following surgery and RCT: high levels of staining for a protein called Hsp70 in tumor cells, and low numbers of tumor-infiltrating NK lymphocytes. These measures may thus serve as useful prognostic biomarkers for predicting the response of SCCHN to therapy.

#### Introduction

The highly conserved, major stress-inducible Hsp70, also termed HSPA1A, is found in nearly all cellular and subcellular compartments of nucleated cells.<sup>1</sup> Hsp70 fulfills a variety of chaperoning functions, such as maintenance of cellular homeostasis<sup>2,3</sup> by assisting folding, maturation and transport of unfolded proteins, and preventing of apoptosis under stressed and non-stressed conditions.<sup>4,5</sup> Elevated Hsp70 levels are associated with poor prognosis in a variety of tumor entities including osteosarcomas,<sup>6,7</sup> squamous cell carcinoma of the lung,<sup>8</sup> lower rectal cancer and hematological diseases.<sup>9,10</sup> Furthermore, tumor in contrast to normal cells, have also been shown to present Hsp70 on their cell surface.<sup>11,12</sup> Membrane localization of Hsp70 on tumor cells is most likely due to a tumor-specific lipid composition that enables anchorage of Hsp70 in the plasma membrane.<sup>13</sup> Depending on its subcellular localization, Hsp70 can fulfill different tasks; on the one hand, it mediates resistance of tumor cells to RCT,<sup>14</sup> on the other hand, it serves as a recognition structure for a subtype of natural killer (NK) cells that is able to kill highly aggressive, membrane Hsp70-positive tumor cells.<sup>11,15</sup> Based on these results, a protocol has been established to activate this NK cell subpopulation by incubating peripheral blood lymphocytes *ex vivo* with either full length Hsp70 protein, or a peptide derived thereof in combination with low dose IL-2.<sup>16,17</sup> The immune phenotype of Hsp70 peptide plus IL-2 activated NK cells has been determined as CD3<sup>-</sup>CD56<sup>bright</sup>CD94<sup>bright</sup>.<sup>18</sup> Although CD56<sup>bright</sup> NK cells are described to secrete pro-inflammatory

cytokines rather than exerting cytotoxicity, these NK cells are able to efficiently eliminate Hsp70 membrane-positive tumor cells.<sup>18</sup> Safety and tolerability of these *ex vivo* stimulated, autologous NK cells have been demonstrated in a phase I clinical trial.<sup>19</sup> Presently a proof-of-concept phase II randomized clinical trial is ongoing to study the efficacy of *ex vivo* Hsp70-stimulated NK cells in patients with squamous NSCLC in stage IIIA/B after RCT.<sup>8,20</sup>

In our study, which is part of the DTK-ROG initiative, which aims to identify and validate biomarkers for outcome of RCT in SCCHN,<sup>21–26</sup> we aim to study the role of Hsp70 and tumor-infiltrating NK cells as prognostic tumor biomarkers. Every year approximately 500,000 new cases are diagnosed worldwide with SCCHN with 4.8% of total cancer incidence and 4.6% cancer mortality.<sup>27</sup> Apart from tobacco and alcohol, which are considered as main risk factors for the development of head and neck cancer, infection with human papilloma virus (HPV) has been determined as causally connected to oropharyngeal cancer.<sup>28</sup> Due to increasing numbers of HPV infections the incidence for SCCHN is rising especially in younger individuals.<sup>29</sup> Patients with locally advanced SCCHN have a 5 year survival rate of 40–60%.<sup>27</sup> Given the progress in medicine over the last decades these mortality rates are still not satisfying. Consequently, reliable biomarkers, which are able to predict outcome of therapy at an early time point are urgently needed to stratify patients with respect to prognosis and to guide adaptations for the treatment.

An early event in SCCHN carcinogenesis is related to somatic mutations of the protein p16 (chromosome 9p21) that exerts tumor suppressor function by binding to the cyclin D1 CDK4/CDK6 complex, which results in a G1 arrest.<sup>30</sup> Silencing of p16 by homozygous deletion, methylation of the promoter and base pair mutations are associated with a more rapid tumor growth.<sup>31</sup> However, with respect to SCCHN the role of p16, as a prognostic marker for outcome of RCT, remains a matter of debate.<sup>32</sup>

Between 40% and 70% of SCCHN contain mutations in the tumor suppressor gene p53.<sup>33</sup> An accumulation of p53, which can be induced not only by mutations, but also by other mechanisms, results in invasive tumor growth and radioresistance.<sup>34</sup>

Although HPV infection is a risk factor for the development of SCCHN, HPV16 DNA-positive patients show a better clinical outcome compared to their HPV16 DNA-free counterparts.<sup>35</sup> Part of this effect has been attributed to an HPV16-induced activation of the immune system. In line with this finding, infiltration of tumors with CD8<sup>+</sup> cytotoxic T lymphocytes has been found to be associated with an HPV16 DNA-positive status and a favorable tumor prognosis.<sup>25</sup> In addition, higher numbers of CD56<sup>+</sup> tumor-infiltrating NK cells are associated with better prognosis in oropharyngeal squamous cell carcinoma.<sup>36</sup>

In our study, we aimed to assess the role of Hsp70 either alone or in relationship with HPV16 DNA, p16 and p53 status, and the infiltration of tumors with CD56<sup>+</sup> NK cells, as prognostic markers in patients with SCCHN after surgery and RCT.

## Patients and Methods

### SCCHN patients

Between 2004 and 2012, patients with histologically confirmed SCCHN of the oro-, hypopharynx and oral cavity were recruited into the study. Patient characteristics are summarized in Table 1. Apart from pN stage ( $p = 0.020$ ), none of the other clinical parameters summarized in Table 1 show any significant correlation with the Hsp70 status. All patients were treated with radical surgery and postoperative cisplatin-based RCT. The tumor bed and regional lymph nodes have been irradiated with a median dose of 50.4 Gy and a boost up to a total dose of 66 Gy to the former tumor area. Assessment of clinical responses and treatment planning were performed by CT, MRI or PET/CT scans. The follow-up period was at least 24 months.

Formalin-fixed, paraffin-embedded (FFPE) sections were obtained from surgical specimen of the tumor from the oro-, hypopharynx or oral cavity. The oral cavity includes the subsites tongue, floor of mouth, palate and gingival/buccal regions and the oropharynx includes base of the tongue and tonsils. Since this was a multicentre study, the patients were encoded only for the three main anatomic sites oral cavity, oropharynx and hypopharynx. All specimens were centrally acquired together with clinical data, radiotherapy plans, diagnostic images in the

DKTK RadPlanBio Platform at the partner site Dresden. A total of 145 patient tumors in UICC stage IVa,b were analyzed for their expression intensity of Hsp70, and the presence of infiltrating CD56<sup>+</sup> NK cells was analyzed in 114 tumor sections (intraepithelial, stroma, tumor border) by immunohistochemistry (IHC). The total number of patients in the original study was 221,<sup>26</sup> however, serial FFPE sections for Hsp70 staining and NK cell infiltration were available only from 5 (Dresden, Essen, Frankfurt, Munich, Tübingen) DKTK partner sites (Table 1). The multicentre trial was approved by the ethical committees of all 8 DKTK partner sites.

### IHC staining and scoring of Hsp70 intensity in tumor sections

Briefly, serial FFPE sections (4  $\mu$ m) of SCCHN tumor patients ( $N = 145$ ) were prepared and heated by microwaving for 30 min in target retrieval buffer (DAKO, Wientheid, Germany, cat# S1699) to unmask antibody epitopes. Non-specific binding was blocked by incubation in protein blocking solution (5% v/v rabbit serum/antibody diluent (REAL antibody diluent, DAKO cat# S2022) for 60 min. Sections were washed in PBS (Sigma-Aldrich, St Louis, USA) after each step. After an overnight incubation at 4°C with the mouse monoclonal antibody cmHsp70.1 (multi-mune GmbH, Munich, Germany; dilution 1:500 in PBS/1% BSA) and another washing step, sections were incubated with Envision<sup>+</sup> System HRP-labelled anti-mouse polymer (DAKO cat# K4001), followed by a 3,3-diaminobenzidine (DAB<sup>+</sup>) chromogen (DAKO cat# K3468) reaction, which was restricted to exactly 4 min for all staining procedures. Nuclei were counterstained with hematoxylin and eosin (H&E). Then sections were embedded in Eukitt (Sigma cat# 03989) mounting medium. Appropriate quality control and quality assurance procedures were implemented including positive (FaDu) and negative (surrounding tissue) controls run with each assay.

According to the staining intensities tumor sections were scored into the following categories: very weak (score 0), weak (score 1), intermediate (score 2), strong (score 3) and very strong (score 4). Since all nucleated cells contain Hsp70, a very weak staining pattern (score 0) was also observed in surrounding normal tissues. IHC scoring for Hsp70 intensity was performed by three independent, trained evaluators (SS, GM, NT). All scores were blinded to the outcome status for each tumor specimen. At least 5 non-overlapping representative tumor fields were evaluated for each section.

### IHC staining and scoring of the number of tumor-infiltrating CD56<sup>+</sup> NK cells

For the detection of tumor-infiltrating CD56<sup>+</sup> NK cells the mouse monoclonal antibody directed against all isoforms of CD56 (NCAM, clone 1B6 Novocastra, Newcastle upon Tyne, UK) was used. After antigen retrieval, as described above, staining was performed using standardized DAKO Envision FLEX Peroxidase Blocking reagent (DAKO cat# K800) and the antibody directed against CD56 for 120 min at room temperature. After washing, sections ( $N = 114$ ) were incubated with

**Table 1.** Demographic and clinical characteristics of SCCHN patients

	Total				p-Value
	Hsp70 scores 0–2	%	Hsp70 scores 3–4	%	
Gender					0.922
Male	65	44.8	57	39.3	
Female	12	8.3	11	7.6	
Age (mean ± SD)	56.3 ± 10.3		58.1 ± 7.7		0.232
Tumor site					0.318
Oropharynx	44	30.3	43	29.7	
Hypopharynx	9	6.2	11	7.6	
Oral cavity	24	16.6	14	9.6	
pT stage					0.960
1–2	49	33.7	43	29.7	
3–4	28	19.3	25	17.3	
pN stage					<b>0.020*</b>
0–1	24	16.6	10	6.8	
2–3	53	36.5	58	40.1	
Grading					0.771
1	2	1.3	2	1.3	
2	41	28.3	33	22.8	
3	34	23.5	33	22.8	
Resection margin (ECE)					0.717
R0	43	29.7	40	27.5	
R1	34	23.4	28	19.4	
HPV16 DNA					0.277
Positive	25	17.3	28	19.3	
Negative	52	35.8	40	27.6	
p16					0.271
Positive	26	17.9	29	20.1	
Negative	51	35.2	39	26.8	
p53					0.055
Positive	37	25.6	22	15.1	
Negative	40	27.5	46	31.8	
Smoking history					0.570
Yes	68	46.9	62	42.7	
No	9	6.2	6	4.2	
CD56 <sup>+</sup> NK cell infiltration					
Low	15	28.8	13	28.3	
High	37	71.2	33	71.7	

Bold values marked with \* present *p*-values <0.05 and are considered as statistically significant.

Envision<sup>+</sup> System HRP-labelled anti-mouse polymer (DAKO cat# K4001), followed by a DAB<sup>+</sup> chromogen (DAKO cat# K3468) reaction. H&E staining was performed for a visual distinction of the tumor and its microenvironment. All sections were embedded in Eukitt (Sigma cat# 03989) mounting medium.

The number of infiltrating CD56<sup>+</sup> NK cells was determined by counting of at least five different compartments of the tumor

and its microenvironment within an area of at least 0.1 mm<sup>2</sup> per slide. The counting of the NK cells was performed at a magnification of ×400. The NK cell counts were determined blinded by three-independent researchers (SS, GM, NT).

The total numbers within one area of interest ranged from 0 to 2,000 NK cells within the tumor and its microenvironment. The median number of infiltrating NK cells in an



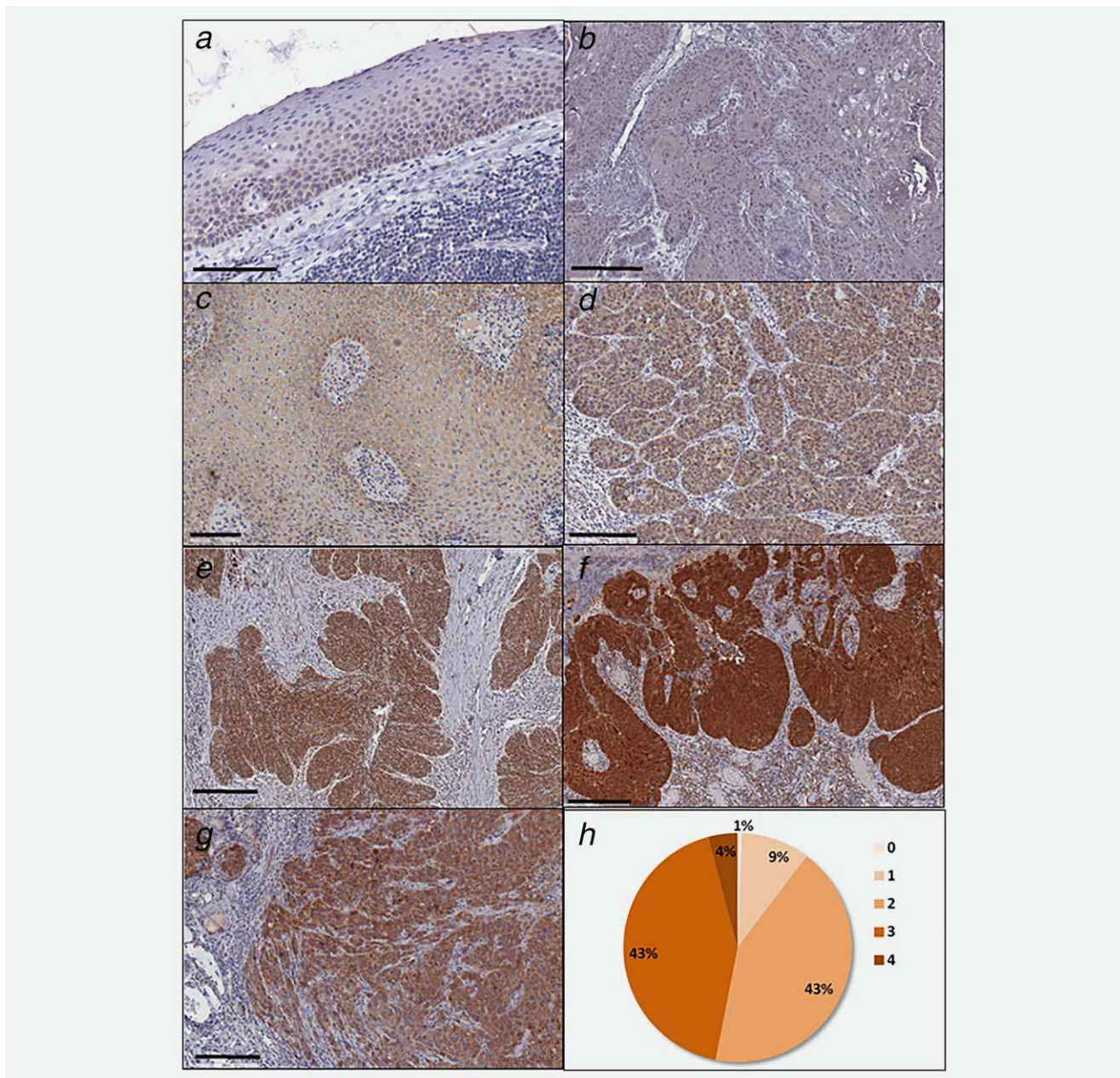


**Figure 1.** Representative views of the Hsp70 expression in normal epithelial tissue of the head and neck (*a*: score 0), and SCCHN tissue with very weak (*b*: score 0), weak (*c*: score 1), intermediate (*d*: score 2), strong (*e*: score 3) and very strong (*f*: score 4) staining intensity. As an internal control the staining intensity of a xenograft FaDu tumor is shown (*g*). The distribution of the different staining scores (0–4) in all 145 tumor sections is represented in (*h*).

individual area was calculated. The cut-off point of 50 NK cells was chosen based on visual inspection of all sections. In sections with <50 events the localization of infiltrating NK cells was disperse, whereas sections with >50 events showed a more dense localization of NK cells.

#### HPV16, p16, p53 analysis

The analysis of the HPV16 status as well as the p16 and p53 staining was performed centrally at the DTKK partner site Dresden. The HPV analysis and genotyping were performed

by using the LCD-Assay HPV-array HPV 3.5 Kit (Chiron GmbH) after extraction of the genomic DNA, as described previously.<sup>28</sup> IHC staining for p16 was performed with the CINtec Immunohistology Kit (Roche). A p16-positive phenotype was defined if at least 70% of the sample was stained positively as determined by two-independent researchers.<sup>28</sup>

#### Statistics

Distributions of categorical variables within the groups of patients with low and high Hsp70 scores are described by

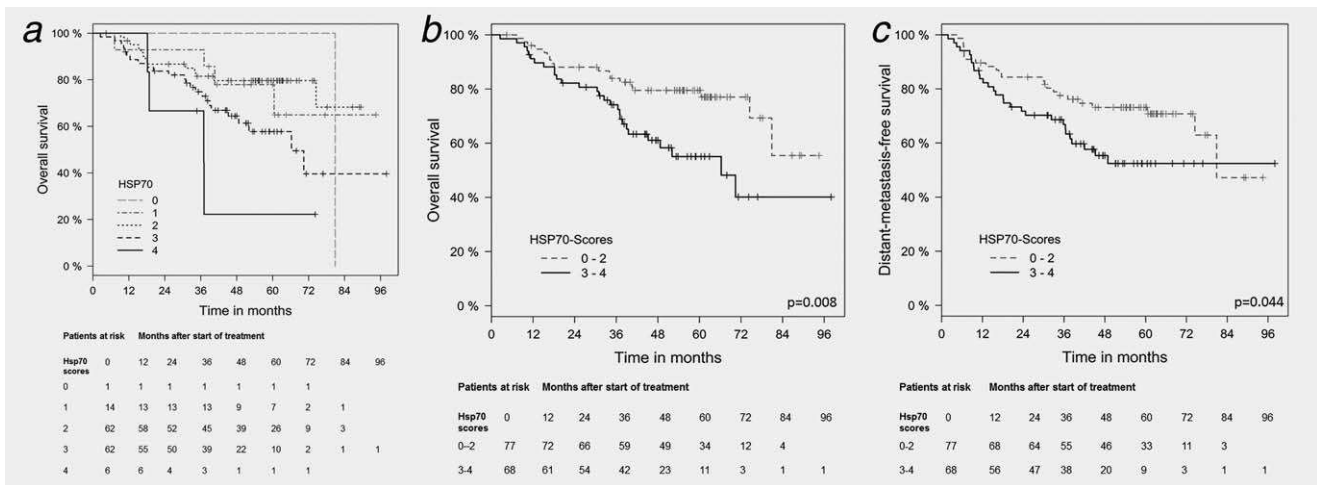


**Figure 2.** Kaplan–Meier analysis of the prognostic value of Hsp70 expression (scores 0–4) with overall survival (OS) and distant metastases-free survival (DMFS). (a) Increasing Hsp70 expression (scores 0–4) in FFPE tumor sections of SCCHN patients ( $N = 145$ ) is associated with sequentially decreased OS. Patients at risk with Hsp70 scores 0–4 at the different time-points after start of therapy ranging from 0 to 96 months are indicated below. (b) Significant correlation of a low (scores 0–2;  $N = 77$ ) vs. high (scores 3–4;  $N = 68$ ) Hsp70 expression in FFPE tumor sections of SCCHN patients with OS. Patients at risk with Hsp70 scores 0–2 vs. 3–4 at different time-points after start of therapy ranging from 0 to 96 months are indicated below the graph. (c) Significant correlation of a low (scores 0–2) vs. high (scores 3–4) Hsp70 expression in FFPE tumor sections of SCCHN patients with DMFS. Patients at risk with Hsp70 scores 0–2 vs. 3–4 at different time-points after start of therapy ranging from 0 to 96 months are indicated below the graph.

**Table 2.** Univariate and multivariate analysis of Hsp70 and other relevant variables as prognostic factors for overall survival (OS)

	Univariate				Multivariate			
	HR	CI <sub>low</sub>	CI <sub>upp</sub>	<i>p</i> -Value	HR	CI <sub>low</sub>	CI <sub>upp</sub>	<i>p</i> -Value
Hsp70 (scores 3–4 vs. 0–2)	2.26	1.24	4.12	<b>0.008*</b>	3.62	1.89	6.92	<b>0.0001*</b>
Age	0.98	0.96	1.01	0.232				
Gender (female vs. male)	1.24	0.70	2.20	0.454				
Tumor site				<b>0.001*</b>				0.072
Oropharynx vs. oral cavity	0.40	0.24	0.66	<b>0.0004*</b>	0.66	0.33	1.33	0.244
Hypopharynx vs. oral cavity	0.33	0.15	0.73	<b>0.006*</b>	0.32	0.12	0.86	<b>0.023*</b>
pT stage (3–4 vs. 1–2)	2.20	1.37	3.52	<b>0.001*</b>	2.00	1.09	3.65	<b>0.024*</b>
pN stage (2–3 vs. 0–1)	1.09	0.63	1.89	0.747				
Grading (3 vs. 1–2)	0.79	0.49	1.28	0.341				
Resection margin (ECE)	1.72	1.06	2.80	<b>0.030*</b>	2.53	1.28	4.99	<b>0.008*</b>
HPV16 DNA (pos vs. neg)	0.33	0.17	0.62	<b>0.0007*</b>	0.24	0.08	0.71	<b>0.010*</b>
p16 (pos vs. neg)	0.39	0.22	0.70	<b>0.002*</b>	0.51	0.20	1.29	0.155
p53 (pos vs. neg)	1.67	1.04	2.67	<b>0.033*</b>	0.69	0.36	1.33	0.265
Smoking history (yes vs. no)	0.80	0.54	1.17	0.250				

Abbreviations: HR, hazard ratio; CI<sub>low/upp</sub>, lower and upper 95% confidence interval.

Bold values marked with \* present *p*-values <0.05 and are considered as statistically significant.

absolute and relative frequencies. For comparisons of these distributions chi-squared tests were performed. For patients' age at diagnosis means and standard deviations are given. Comparisons of the mean were conducted using a two-sample *t*-test.

Overall survival (OS), distant metastases-free survival (DMFS) and local progression-free survival (LPFS) were calculated from the start of RCT to the day of death. Kaplan–

Meier curves are presented for relevant outcomes and groups. Log Rank tests were performed to compare distributions of event times between patients with low and high Hsp70 scores. In addition, univariate Cox regression models were used to determine hazard ratios (HRs) and 95% confidence intervals (CIs). To assess the additional prognostic value of Hsp70 to other prognostic factors,<sup>37</sup> multivariable Cox regression models including Hsp70 and relevant prognostic

**Table 3.** Univariate and multivariate analysis of Hsp70 and other relevant variables as prognostic factors for local progression-free survival (LPFS)

	Univariate				Multivariate			
	HR	CI <sub>low</sub>	CI <sub>upp</sub>	p-Value	HR	CI <sub>low</sub>	CI <sub>upp</sub>	p-Value
Hsp70 (scores 3–4 vs. 0–2)	1.84	1.05	3.22	<b>0.034*</b>	2.63	1.45	4.78	<b>0.002*</b>
Age	0.98	0.96	1.01	0.180				
Gender (female vs. male)	1.54	0.90	2.61	0.113				
Tumor site				<b>&lt;0.001*</b>				0.088
Oropharynx vs. oral cavity	0.39	0.24	0.64	<b>0.0002*</b>	0.63	0.32	1.22	0.172
Hypopharynx vs. oral cavity	0.35	0.17	0.75	<b>0.006*</b>	0.39	0.16	0.97	<b>0.042*</b>
pT stage (3–4 vs. 1–2)	2.23	1.42	3.52	<b>0.0005*</b>	1.94	1.09	3.44	<b>0.022*</b>
pN stage (2–3 vs. 0–1)	1.10	0.65	1.87	0.730				
Grading (3 vs. 1–2)	0.75	0.47	1.21	0.243				
Resection margin (ECE)	1.60	1.00	2.54	0.050	1.97	1.05	3.70	<b>0.035*</b>
HPV16 DNA (pos vs. neg)	0.33	0.18	0.61	<b>0.0004*</b>	0.32	0.12	0.88	<b>0.028*</b>
p16 (pos vs. neg)	0.38	0.22	0.67	<b>0.0008*</b>	0.53	0.22	1.28	0.158
p53 (pos vs. neg)	1.86	1.18	2.92	<b>0.007*</b>	0.90	0.48	1.68	0.774
Smoking history (yes vs. no)	0.84	0.58	1.22	0.368				

Abbreviations: HR, hazard ratio; CI<sub>low/upp</sub>, lower and upper 95% confidence interval.

Bold values marked with \* present *p*-values <0.05 and are considered as statistically significant.

**Table 4.** Univariate and multivariate analysis of Hsp70 and other relevant variables as prognostic factors for distant metastases-free survival (DMFS)

	Univariate				Multivariate			
	HR	CI <sub>low</sub>	CI <sub>upp</sub>	p-Value	HR	CI <sub>low</sub>	CI <sub>upp</sub>	p-Value
Hsp70 (scores 3–4 vs. 0–2)	1.76	1.01	3.07	<b>0.044*</b>	2.42	1.34	4.37	<b>0.003*</b>
Age	0.99	0.97	1.02	0.443				
Gender (female vs. male)	1.06	0.60	1.86	0.842				
Tumor site				<b>0.001*</b>				0.629
Oropharynx vs. oral cavity	0.40	0.25	0.65	<b>0.0002*</b>	0.73	0.37	1.42	0.350
Hypopharynx vs. oral cavity	0.55	0.28	1.08	0.081	0.88	0.39	2.01	0.763
pT stage (3–4 vs. 1–2)	2.19	1.39	3.42	<b>0.0006*</b>	1.90	1.09	3.31	<b>0.024*</b>
pN stage (2–3 vs. 0–1)	1.26	0.73	2.14	0.425				
Grading (3 vs. 1–2)	0.87	0.55	1.38	0.563				
Resection margin (ECE)	1.89	1.18	3.01	<b>0.008*</b>	2.51	1.33	4.75	<b>0.005*</b>
HPV16 DNA (pos vs. neg)	0.35	0.19	0.63	<b>0.0005*</b>	0.35	0.13	0.97	<b>0.044*</b>
p16 (pos vs. neg)	0.36	0.20	0.63	<b>0.0002*</b>	0.44	0.18	1.10	0.080
p53 (pos vs. neg)	1.78	1.14	2.78	<b>0.012*</b>	0.86	0.46	1.60	0.631
Smoking history (yes vs. no)	0.81	0.56	1.17	0.261				

Abbreviations: HR, hazard ratio; CI<sub>low/upp</sub>, lower and upper 95% confidence interval.

Bold values marked with \* present *p*-values <0.05 and are considered as statistically significant.

factors were fit to the data for overall survival (OS), local progression-free survival (LPFS) and distant metastases-free survival (DMFS). Median follow-up time was determined using the reverse Kaplan–Meier method for potential follow-up.<sup>38</sup> All statistical tests were performed two-sided on a significance level of  $\alpha = 5\%$ . Analyses were performed with statistical software R version 3.3.2<sup>39</sup> and IBM SPSS Statistics for Windows, version 23 and 24 (IBM Corp, Armonk, NY).

## Results

### Hsp70 staining intensities in FFPE sections of SCCHN

An incubation of SCCHN tumor sections and the surrounding tissue with cmHsp70.1 monoclonal antibody (mAb) revealed significant differences in the staining intensity. The surrounding epithelial tissue in close proximity to the tumor (Fig. 1b) always showed a very weak staining intensity (score 0), which is comparable to that of normal head and neck



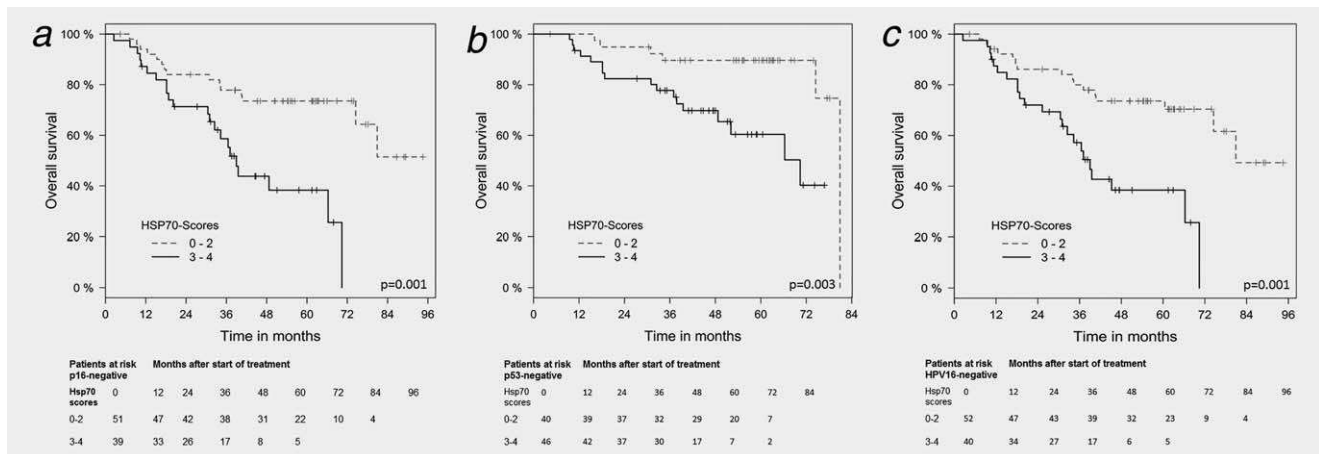


**Figure 3.** Kaplan-Meier analysis of the prognostic value of Hsp70 expression (scores 0–2 vs. 3–4) and overall survival (OS) in subgroups of patients with p16-, p53- and HPV16 DNA-negative tumors. (a) Significant correlation of a low (scores 0–2) vs. high (scores 3–4) Hsp70 expression in FFPE tumor sections of SCCHN patients with p16-negative tumors ( $N = 90$ ) and OS. Patients at risk with Hsp70 scores 0–2 vs. 3–4 and a p16-negative status at different time-points after start of therapy ranging from 0 to 96 months are indicated below the graph. (b) Significant correlation of a low (scores 0–2) vs. high (scores 3–4) Hsp70 expression in FFPE tumor sections of SCCHN patients with p53-negative tumors ( $N = 86$ ) and OS. Patients at risk with Hsp70 scores 0–2 vs. 3–4 and a p53-negative status at different time-points after start of therapy ranging from 0 to 84 months are indicated below the graph. (c) Significant correlation of a low (scores 0–2) vs. high (scores 3–4) Hsp70 expression in FFPE tumor sections of SCCHN patients with HPV16 DNA-negative tumors ( $N = 92$ ) and OS. Patients at risk with Hsp70 scores 0–2 vs. 3–4 and a HPV16 DNA-negative status at different time-points after start of therapy ranging from 0 to 96 months are indicated below the graph.

epithelial tissue (Fig. 1a). Representative FFPE tumor sections of different patients stained with cmHsp70.1 mAb are shown in Figures 1b–1f. According to their Hsp70 expression, tumors were scored into groups with very weak to weak (scores 0–1; Figs. 1b and 1c), intermediate (score 2; Fig. 1d), strong (score 3; Fig. 1e) and very strong (score 4; Fig. 1f) staining intensity. As an internal reference FFPE sections of xenograft FaDu tumors were co-stained with each staining procedure (Fig. 1g). The percentage of tumor sections with a specific staining scores (0–4) are summarized in Figure 1h.

#### Correlation of the Hsp70 staining intensity with OS, LPFS and DMFS

To determine the prognostic value of the Hsp70 expression in relation to OS different Hsp70 staining scores ranging from very weak (0) to very strong (4) have been compared. As summarized in Figure 2a, increasing Hsp70 scores are associated with an increased mortality. Regarding a dichotomous variable, SCCHN with high Hsp70 staining intensities (scores 3–4, black line) exhibited a significantly lower overall survival (OS; HR = 2.26,  $p = 0.008$ ; Fig. 2b, Table 2), local progression-free survival (LPFS; HR = 1.84,  $p = 0.034$ ; Table 3) and distant metastases-free (DMFS; HR = 1.76,  $p = 0.044$ ; Fig. 2c, Table 4) than patients with low Hsp70 tumor staining intensity (scores 0–2, gray line). Patients at risk at the different time-points after start of therapy are shown below each graph. Multivariate analyses of Hsp70 staining intensities after adjustment for other relevant prognostic parameters with OS (Table 2), LPFS (Table 3) and DMFS (Table 4) revealed similar significant results.

In a subgroup analysis, the staining intensity of Hsp70 within the tumor was also assessed in combination with the p16, p53 and HPV16 status. Patients with p16-negative ( $N = 90$ ;  $p = 0.001$ ) and p53-negative ( $N = 59$ ;  $p = 0.003$ ) tumors presented a significantly better clinical outcome with respect to OS when the Hsp70 tumor staining intensity was low (scores 0–2, gray line) compared to those with a high (scores 3–4, black line) Hsp70 tumor staining intensity (Figs. 3a and 3b). With respect to HPV16, virus DNA-free patients with a low Hsp70 staining intensity (scores 0–2, gray line) also showed a significantly improved overall survival ( $N = 92$ ;  $p = 0.001$ ) compared to those patients with a high tumor staining intensity (scores 3–4, black line; Fig. 3c).

In summary, a strong Hsp70 staining intensity of the tumor could be identified as an independent negative prognostic factor for OS, freedom of metastases and locoregional control in patients with SCCHN. The negative prognostic value of a strong Hsp70 expression was also observed in patient cohorts with a p16-, p53-, HPV16 DNA-negative tumors that are known to have an adverse prognosis.

#### Infiltration of CD56<sup>+</sup> NK cells in FFPE sections of SCCHN

Since membrane Hsp70 serves as a target for activated NK cells,<sup>17</sup> showing a high expression density of the NK marker CD56,<sup>40</sup> a CD56-specific antibody was used to determine the amount of tumor-infiltrating NK cells. A representative view of tumors with high (upper graph) and low (lower graph) NK cell infiltration is shown in Figure 4a. White arrows mark the localization of either singular or multiple CD56<sup>+</sup> NK cell infiltrations within the tumor and its microenvironment. The data

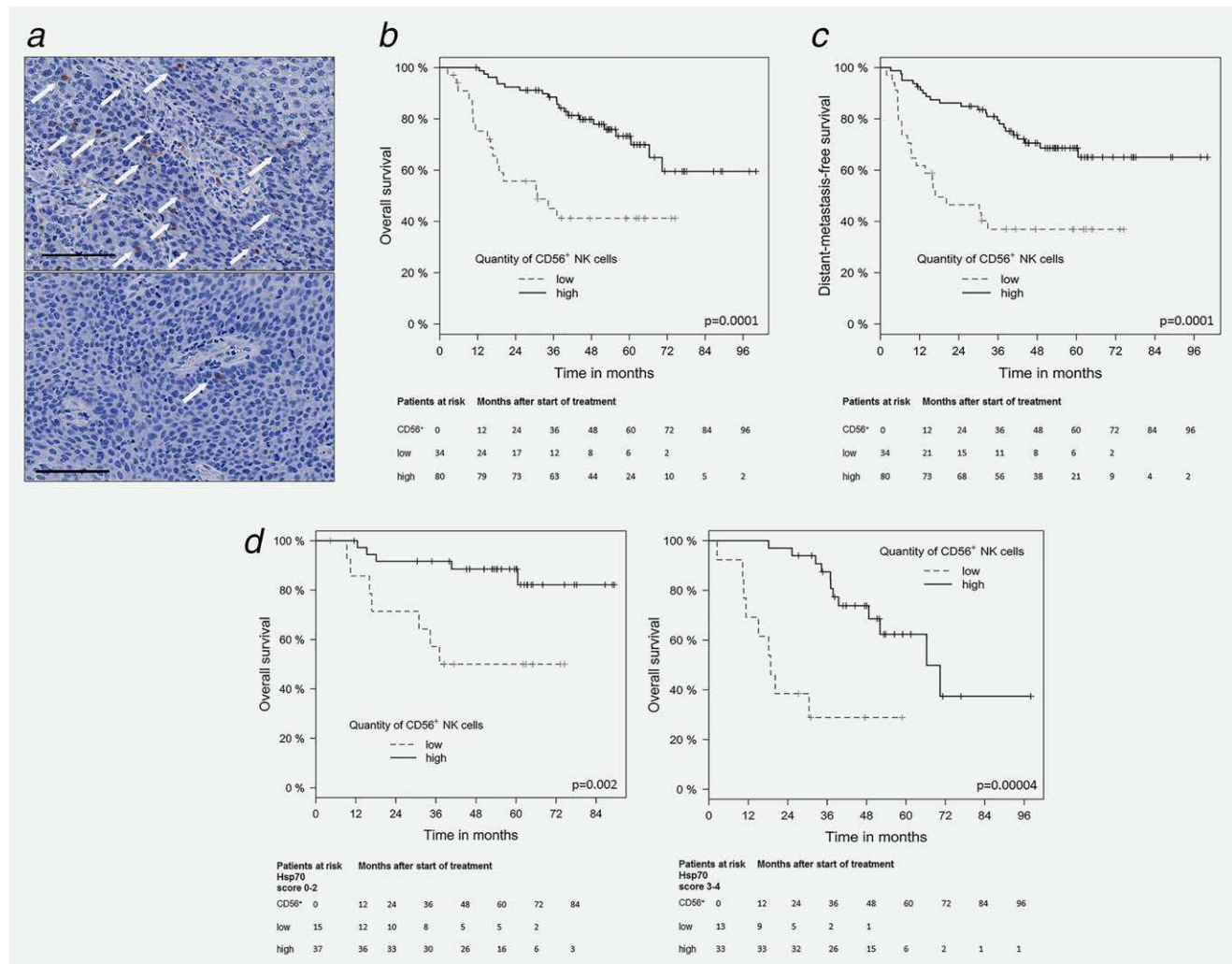


**Figure 4.** Kaplan–Meier analysis of the prognostic value of infiltrating CD56<sup>+</sup> NK cells in FFPE tumor sections of SCCHN patients with overall survival (OS) and distant metastases-free survival (DMFS). (a) Representative view of SCCHN sections with high (upper graph) and low numbers (lower graph) of infiltrating CD56<sup>+</sup> NK cells. Selected singular as well as groups of CD56<sup>+</sup> NK cells are marked with white arrows, scale bar, 100 μm. (b) Significant correlation of infiltrating CD56<sup>+</sup> NK cells in tumor sections of SCCHN patients (N = 114) and OS. Black line represents high and gray lines represent low numbers of infiltrating CD56<sup>+</sup> NK cells. Patients at risk with low and high numbers of infiltrating CD56<sup>+</sup> NK cells at different time-points after start of therapy ranging from 0 to 96 months are indicated below the graph. (c) Significant correlation of infiltrating CD56<sup>+</sup> NK cells in tumor sections of SCCHN patients (N = 114) and DMFS. Black line represents high and gray lines represent low numbers of infiltrating CD56<sup>+</sup> NK cells. Patients at risk with low and high numbers of infiltrating CD56<sup>+</sup> NK cells at different time-points after start of therapy ranging from 0 to 96 months are indicated below the graph. (d) Significant correlation of infiltrating CD56<sup>+</sup> NK cells in tumor sections with low (left graph; scores 0–2) and high Hsp70 expression (right graph, scores of 3–4) and OS. Patients at risk with low and high numbers of infiltrating CD56<sup>+</sup> NK cells and an Hsp70 scores of 0–2 vs. 3–4 at different time-points after start of therapy ranging from 0 to 84 and 0 to 96 months are indicated below the graph are indicated below each graph. (e) Representative views of serial FFPE sections of tumors with an Hsp70 score of 2 (left graph) and a low number of infiltrating NK cells and an Hsp70 score of 4 (right graph) and a high number of infiltrating NK cells. The insets show a 400× magnification. (f) Significant correlation of tumor-infiltrating CD56<sup>+</sup> NK cells in tumor sections with low (left graph; scores of 0–2) vs. high Hsp70 expression (right graph; scores of 3–4) and DMFS. Patients at risk with low and high numbers of infiltrating CD56<sup>+</sup> NK cells and an Hsp70 scores of 0–2 vs. 3–4 at different time-points after start of therapy ranging from 0 to 84 and 0 to 96 months are indicated below the graph are indicated below each graph.

shown in Figure 4b and Table 5 clearly indicate that low numbers of CD56<sup>+</sup> tumor-infiltrating NK cells have a negative prognostic value for a significantly decreased OS in patients with SCCHN (HR = 0.29, p = 0.0001). Comparable results were obtained for LPFS (HR = 0.35, p = 0.0009) as shown in Table 6. As illustrated in Figure 4c and Table 7, distant

metastases develop significantly earlier in patients with a low tumor-infiltration of CD56<sup>+</sup> NK cells (HR = 0.31, p = 0.0001).

Similar results are found in subgroup analysis of tumors with low (scores 0–2) and high Hsp70 expression (scores 3–4). As shown in Figure 4d, low numbers of CD56<sup>+</sup> tumor-infiltrating NK cells in tumor sections with low (left graph; scores 0–2,



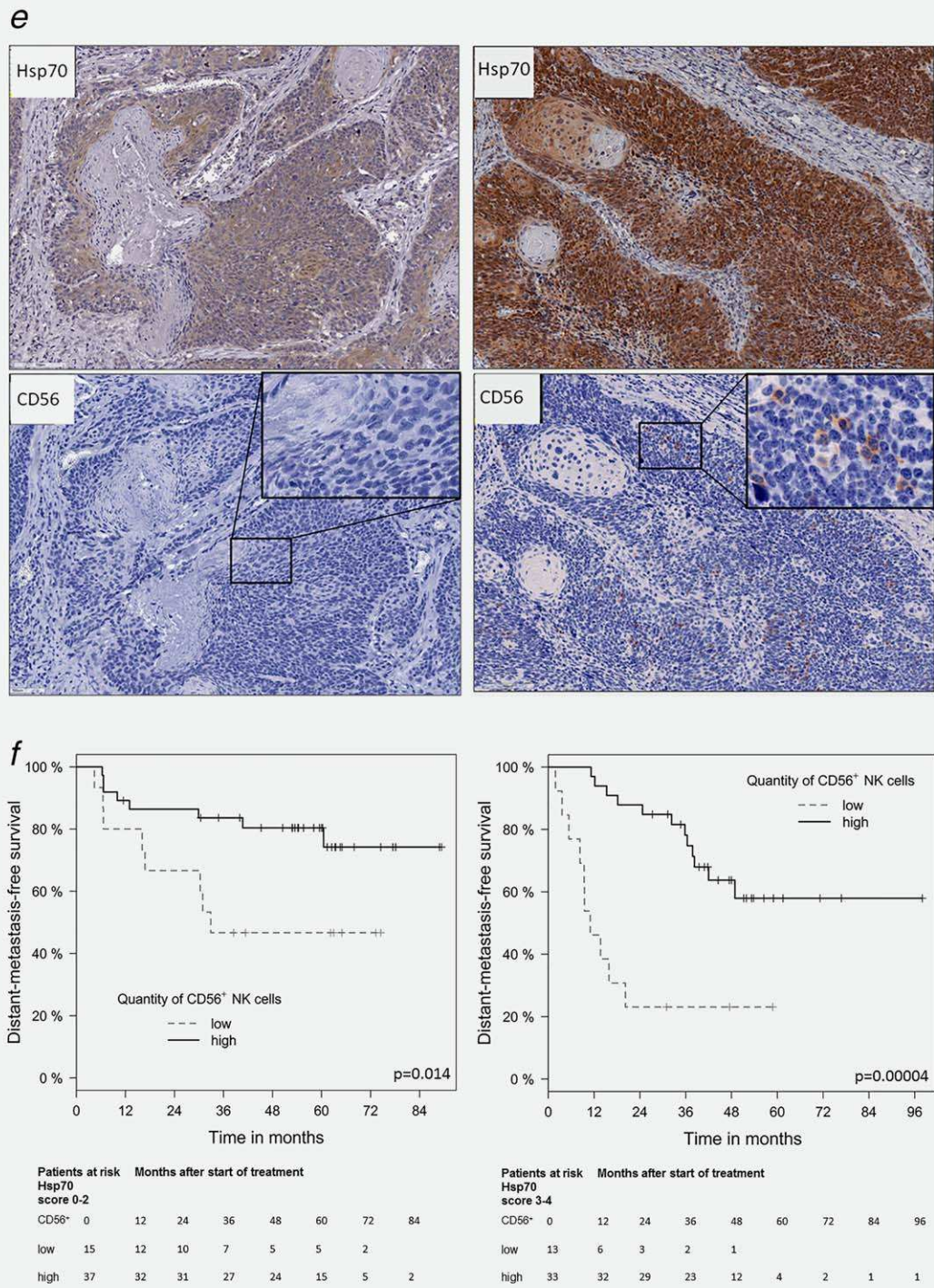


Figure 4. Continued.

*p* = 0.002) and high (right graph; scores 3–4, *p* = 0.00004) Hsp70 expression correlate with significantly decreased OS. Representative views of serial sections of tumors with low (score 2,

upper left graph) and high (score 4, upper right graph) Hsp70 expression and a low (lower left graph) and high (lower right graph) NK cell infiltration are illustrated in Figure 4e.

**Table 5.** Univariate and multivariate analysis of tumor-infiltrating CD56<sup>+</sup> NK cells and other relevant variables as prognostic factors for overall survival (OS)

	Univariate				Multivariate			
	HR	CI <sub>low</sub>	CI <sub>upp</sub>	<i>p</i> -Value	HR	CI <sub>low</sub>	CI <sub>upp</sub>	<i>p</i> -Value
CD56 (high vs. low)	0.29	0.15	0.55	<b>0.0001*</b>	0.27	0.12	0.60	<b>0.001*</b>
Tumor site								
Oropharynx vs. oral cavity					0.86	0.35	2.07	0.732
Hypopharynx vs. oral cavity					0.56	0.15	2.05	0.381
pT stage (3–4 vs. 1–2)					2.33	1.12	4.79	<b>0.022*</b>
Resection margin (ECE)					2.28	0.92	5.65	0.075
HPV16 DNA (pos vs. neg)					0.29	0.07	1.10	0.070
p16 (pos vs. neg)					0.60	0.20	1.85	0.377
p53 (pos vs. neg)					1.06	0.46	2.48	0.885

Abbreviations: HR, hazard ratio; CI<sub>low/upp</sub>, lower and upper 95% confidence interval.  
 Bold values marked with \* present *p*-values <0.05 and are considered as statistically significant.

**Table 6.** Univariate and multivariate analysis of tumor-infiltrating CD56<sup>+</sup> NK cells and other relevant variables as prognostic factors for local progression-free survival (LPFS)

	Univariate				Multivariate			
	HR	CI <sub>low</sub>	CI <sub>upp</sub>	<i>p</i> -Value	HR	CI <sub>low</sub>	CI <sub>upp</sub>	<i>p</i> -Value
CD56 (high vs. low)	0.35	0.19	0.65	<b>0.0009*</b>	0.35	0.17	0.74	<b>0.005*</b>
Tumor site								
Oropharynx vs. oral cavity					0.77	0.32	1.79	0.547
Hypopharynx vs. oral cavity					0.62	0.19	2.02	0.430
pT stage (3–4 vs. 1–2)					2.26	1.13	4.53	<b>0.021*</b>
Resection margin (ECE)					1.63	0.72	3.74	0.241
HPV16 DNA (pos vs. neg)					0.38	0.11	1.33	0.130
p16 (pos vs. neg)					0.68	0.24	1.95	0.477
p53 (pos vs. neg)					1.39	0.61	3.15	0.437

Abbreviations: HR, hazard ratio; CI<sub>low/upp</sub>, lower and upper 95% confidence interval.  
 Bold values marked with \* present *p*-values <0.05 and are considered as statistically significant.

**Table 7.** Univariate and multivariate analysis of tumor-infiltrating CD56<sup>+</sup> NK cells and other relevant variables as prognostic factors for distant metastases-free survival (DMFS)

	Univariate				Multivariate			
	HR	CI <sub>low</sub>	CI <sub>upp</sub>	<i>p</i> -Value	HR	CI <sub>low</sub>	CI <sub>upp</sub>	<i>p</i> -Value
CD56 (high vs. low)	0.31	0.17	0.57	<b>0.0001</b>	0.27	0.13	0.55	<b>0.0004*</b>
Tumor site								
Oropharynx vs. oral cavity					0.75	0.33	1.70	0.489
Hypopharynx vs. oral cavity					2.43	0.76	7.74	0.135
pT stage (3–4 vs. 1–2)					2.06	1.05	4.06	<b>0.036*</b>
Resection margin (ECE)					2.35	1.02	5.42	<b>0.044*</b>
HPV16 DNA (pos vs. neg)					0.57	0.17	1.95	0.370
p16 (pos vs. neg)					0.49	0.17	1.40	0.184
p53 (pos vs. neg)					1.66	0.73	3.75	0.227

Abbreviations: HR, hazard ratio; CI<sub>low/upp</sub>, lower and upper 95% confidence interval.  
 Bold values marked with \* present *p*-values <0.05 and are considered as statistically significant.



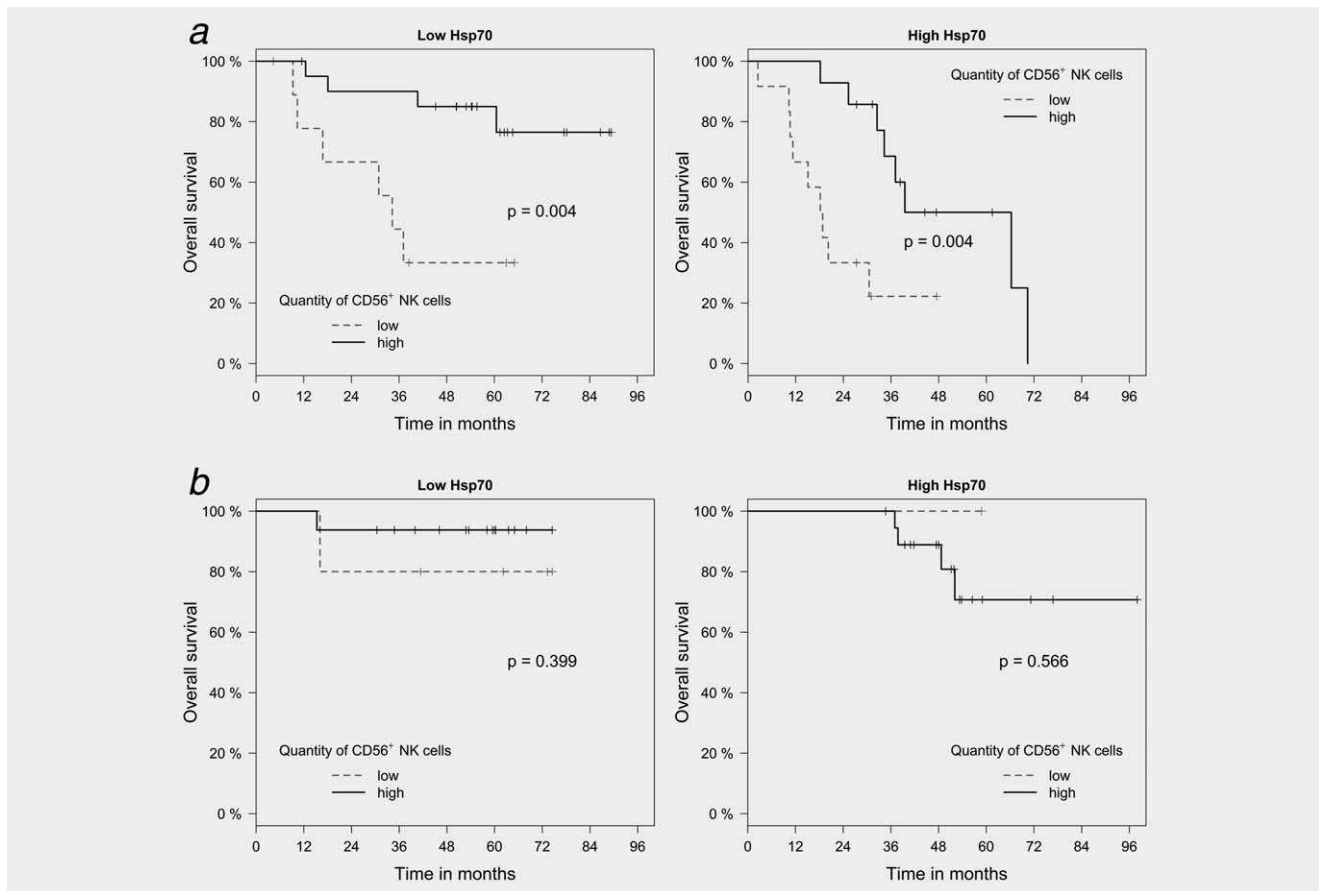


**Figure 5.** Kaplan–Meier analysis of the prognostic value of the CD56<sup>+</sup> NK cell/Hsp70 marker combination in FFPE tumor sections of HPV16 DNA-negative ( $N = 92$ ) and -positive ( $N = 53$ ) SCCHN patients with overall survival (OS). (a) Significant correlation of infiltrating CD56<sup>+</sup> NK cells in tumor sections of HPV16 DNA-negative SCCHN patients ( $N = 92$ ) and OS in sections with a low (scores 0–2,  $p = 0.004$ ) and high (scores 3–4,  $p = 0.004$ ) Hsp70 expression. Black line represents high and gray lines represent low numbers of infiltrating CD56<sup>+</sup> NK cells. (b) No significant correlation of infiltrating CD56<sup>+</sup> NK cells in tumor sections of HPV16 DNA-positive SCCHN patients ( $N = 53$ ) and OS in sections with a low (scores 0–2) and high (scores 3–4) Hsp70 expression. Black line represents high and gray lines represent low numbers of infiltrating CD56<sup>+</sup> NK cells.

Low numbers of tumor-infiltrating CD56<sup>+</sup> NK cells also correlate with a significantly shorter DMFS, as shown in Figure 4f. The combination of a high Hsp70 expression (scores 3–4) and a low NK cell infiltration shows better negative prognostic value ( $p = 0.0004$ ; Fig. 4f, right graph) than a low Hsp70 expression (scores 0–2) and a low NK cell infiltration ( $p = 0.014$ ; Fig. 4f, left graph) although both values were statistical significant.

Univariate and multivariate analysis of tumor-infiltrating CD56<sup>+</sup> NK cells in combination with OS (Table 5), LPFS (Table 6) and DMFS (Table 7) revealed that both markers Hsp70 and NK cells have prognostic value.

Analysis of the prognostic value of the CD56/Hsp70 marker combination in patients with differential HPV16 status revealed that a high NK cell infiltration positively correlated with an improved OS in HPV16 DNA-negative ( $N = 92$ ,  $p = 0.004$ ; Fig. 5a), but not in HPV16 DNA-positive ( $N = 53$ ; Fig. 5b) patient cohort, irrespective of the Hsp70 status. The lack of statistical significance in the HPV16 DNA-positive patient cohort might be explained by the low number of patients per subgroup.

## Discussion

The search for tumor-specific biomarkers that are frequently overexpressed in malignantly transformed cells resulted in the identification of the highly conserved, major stress-inducible Hsp70.<sup>41</sup> Apart from elevated cytosolic expression levels and in contrast to normal cells, tumor cells frequently present Hsp70 on their cell surface.<sup>11,12,42</sup> It is well accepted that high cytosolic<sup>43</sup> and membrane<sup>14</sup> expression levels of Hsp70 are associated with resistance to therapy and thus might increase tumorigenesis. Previous work has indicated that Hsp70 is also expressed on the membrane of SCCHN.<sup>44</sup> In our study, we addressed the question of the role of cytosolic Hsp70 as a prognostic tumor marker in patients with SCCHN after surgery and postoperative radiotherapy.

To directly compare the Hsp70 staining intensity in different tumors, FFPE sections with identical thickness (4  $\mu\text{m}$ ) have to be stained using the exact same staining protocol together with an internal reference. A comparison of the Hsp70 expression in all SCCHN sections following this procedure revealed major differences in the Hsp70 staining

intensity ranging from very weak to very strong. Our data suggest that an accumulation of Hsp70 within the tumor tissue positively correlates with a decreased OS, PFS and DMFS after surgery and RCT. Therefore, a high Hsp70 expression serves as a negative prognostic marker for patients with SCCHN. This negative prognostic value of Hsp70 is in line with reports demonstrating anti-apoptotic and pro-tumorigenic activities for Hsp70.<sup>43,45</sup>

Every nucleated cell type expresses Hsp70 at low levels in the cytosol, but nearly all tumor types show a significantly enhanced Hsp70 expression. Therefore, normal tissues as well as the tumor microenvironment cannot be expected to be completely negative for Hsp70.

A comparison of membrane-bound and cytosolic Hsp70 levels in tumor cells revealed that approximately 70–90% of the total Hsp70 is residing in the cytosol.<sup>41</sup> Together with the finding that cmHsp70.1 mAb<sup>42</sup> detects both, membrane-bound and cytosolic Hsp70, it is not possible to distinguish both localizations in FFPE sections.

A number of studies indicated that a HPV16 DNA-positive status is associated with favorable outcome,<sup>46</sup> although HPV16 has been determined as a co-founding factor that can initiate SCCHN. This finding might be related to the immunostimulatory activity of the virus to induce anti-tumor-specific immune responses. However, a positive correlation of HPV16 has also been found between CTLA-4 expression, Treg infiltration and HPV16 DNA positivity, which might exert immunosuppressive effects.<sup>47</sup> Therefore, in combination with RCT blocking of immune checkpoint inhibitors might be beneficial to overcome immunosuppression in SCCHN. Apart from an involvement of the immune system additional factors such as smaller tumor size, lower amount of CD44<sup>+</sup>/CD98<sup>+</sup> tumor stem cells,<sup>48</sup> higher sensitivity to RCT,<sup>26</sup> less tumor hypoxia, (E6)-induced inhibition of p53,<sup>49,50</sup> younger patient age and less toxin (tobacco, alcohol) intake are also involved in a favorable outcome.<sup>26,36</sup>

We also could demonstrate that in patients with HPV16 DNA-free tumors the Hsp70 staining intensity still could separate two subgroups with respect to outcome. Patients with HPV16-negative tumors and low Hsp70 staining intensity (scores 0–2) showed a significantly improved OS compared to those with a high Hsp70 staining intensity (scores 3–4).

With respect to the p16 and p53 status,<sup>30–32</sup> patients with p16- ( $N=90$ ) and p53-negative SCCHN tumors presented a significantly worse clinical outcome when the Hsp70 tumor staining intensity was high. Therefore, we assume that Hsp70 in addition to p16 and p53 might provide additional prognostic value.

Depending on the subcellular, membrane-bound and extracellular localization Hsp70 mediates different functions.

However, it is worth mentioning that the membrane status of Hsp70 cannot be determined by IHC, since most tumor cells show a very strong Hsp70 cytosolic staining<sup>41</sup> that does not allow to detect the faint membrane staining pattern in FFPE sections. Despite these limitations, we addressed the question whether a strong cytosolic Hsp70 expression might affect infiltration of CD56<sup>+</sup> NK cells into the tumor tissue and whether a strong infiltration of NK cells might also be associated with favorable clinical outcome, as previously shown for CD8<sup>+</sup> cytotoxic lymphocytes.<sup>25</sup>

A correlation of OS with high numbers of infiltrating NK cells supports the hypothesis that apart from the adaptive also the innate immune system plays an important role in the outcome of surgery and RCT in SCCHN.<sup>44</sup> Indeed, patients with high numbers of tumor-infiltrating CD56<sup>+</sup> NK cells show superior OS.<sup>36</sup> However, overall life expectancy is significantly lower in the group of patients bearing tumors with high cytosolic Hsp70 levels. This might be explained by high intracellular Hsp70 levels that impair NK cell and RCT-mediated tumor cell apoptosis by inhibiting lysosomal permeabilization.<sup>45</sup> The anti-apoptotic effect of intracellular Hsp70 might overrule beneficial effects mediated by tumor-infiltrating NK cells.

A high number of tumor-infiltrating NK cells results not only in an improved OS but also in DMFS. This finding might be due to the fact that the Hsp70 membrane density is often stronger on metastases compared to primary tumors,<sup>51</sup> and thus might serve as a target for the cytolytic attack by NK cells. In contrast to intracellular Hsp70, membrane-bound and extracellular residing Hsp70 have been found to stimulate anti-tumor immunity.<sup>52</sup> Since normal cells do not present Hsp70 on their cell surface, membrane-bound Hsp70 can serve as a tumor-selective target for Hsp70 peptide-activated NK cells.<sup>16,17</sup> Extracellular Hsp70 released by viable tumor cells<sup>53</sup> that chaperones tumor-derived peptides might be able to stimulate the cytolytic activity of CD8<sup>+</sup> T lymphocytes. A previous study of our group revealed that a high membrane expression of Hsp70 on primary tumor cells correlated with high soluble Hsp70 levels in patients with SCCHN.<sup>54</sup> These data are in line with the finding that high cytosolic Hsp70 levels are associated with a high membrane Hsp70 expression and high soluble Hsp70 levels in primary glioblastoma.<sup>55</sup> In an ongoing prospective study extracellular, membrane-bound and cytosolic Hsp70 levels will be assessed in SCCHN patients by using the lipHsp70 ELISA,<sup>53</sup> flow cytometry and IHC together with the immunophenotype of peripheral blood lymphocytes. Our study will allow a better understanding of the role of Hsp70 as a diagnostic marker and its interaction with the immune system.

## References

1. Kampinga HH, Craig EA. The HSP70 chaperone machinery: J proteins as drivers of functional specificity. *Nat Rev Mol Cell Biol* 2010;11:579–92.
2. Hartl FU, Bracher A, Hayer-Hartl M. Molecular chaperones in protein folding and proteostasis. *Nature* 2011;475:324–32.
3. Mayer MP, Bukau B. Hsp70 chaperones: cellular functions and molecular mechanism. *Cell Mol Life Sci* 2005;62:670–84.



4. Beere HM, Wolf BB, Cain K, et al. Heat-shock protein 70 inhibits apoptosis by preventing recruitment of procaspase-9 to the Apaf-1 apoptosome. *Nat Cell Biol* 2000;2:469–75.
5. Gabai VL, Sherman MY. Invited review: interplay between molecular chaperones and signaling pathways in survival of heat shock. *J Appl Physiol* 2002;92:1743–8.
6. Uozaki H, Ishida T, Kakiuchi C, et al. Expression of heat shock proteins in osteosarcoma and its relationship to prognosis. *Pathol Res Pract* 2000;196:665–73.
7. Asling J, Morrison J, Mutsaers AJ. Targeting HSP70 and GRP78 in canine osteosarcoma cells in combination with doxorubicin chemotherapy. *Cell Stress Chaper* 2016;21:1065–76.
8. Gunther S, Ostheimer C, Stangl S, et al. Correlation of Hsp70 serum levels with gross tumor volume and composition of lymphocyte subpopulations in patients with squamous cell and adeno non-small cell lung cancer. *Front Immunol* 2015;6:556.
9. Pfister K, Radons J, Busch R, et al. Patient survival by Hsp70 membrane phenotype: association with different routes of metastasis. *Cancer* 2007;110:926–35.
10. Steiner K, Graf M, Hecht K, et al. High HSP70-membrane expression on leukemic cells from patients with acute myeloid leukemia is associated with a worse prognosis. *Leukemia* 2006;20:2076–9.
11. Multhoff G, Botzler C, Jennen L, et al. Heat shock protein 72 on tumor cells: a recognition structure for natural killer cells. *J Immunol* 1997;158:4341–50.
12. Multhoff G, Botzler C, Wiesnet M, et al. A stress-inducible 72-kDa heat-shock protein (HSP72) is expressed on the surface of human tumor cells, but not on normal cells. *Int J Cancer* 1995;61:272–9.
13. Gehrman M, Liebisch G, Schmitz G, et al. Tumor-specific Hsp70 plasma membrane localization is enabled by the glycosphingolipid Gb3. *PLoS One* 2008;3:e1925.
14. Murakami N, Kühnel A, Schmid TE, et al. Role of membrane Hsp70 in radiation sensitivity of tumor cells. *Radiat Oncol* 2015;10:149.
15. Multhoff G, Mizzen L, Winchester CC, et al. Heat shock protein 70 (Hsp70) stimulates proliferation and cytolytic activity of natural killer cells. *Exp Hematol* 1999;27:1627–36.
16. Multhoff G, Pfister K, Botzler C, et al. Adoptive transfer of human natural killer cells in mice with severe combined immunodeficiency inhibits growth of Hsp70-expressing tumors. *Int J Cancer* 2000;88:791–7.
17. Multhoff G, Pfister K, Gehrman M, et al. A 14-mer Hsp70 peptide stimulates natural killer (NK) cell activity. *Cell Stress Chaper* 2001;6:337–44.
18. Romagnani C, Juelke K, Falco M, et al. CD56bright/CD16- killer Ig-like receptor-NK cells display longer telomeres and acquire features of CD56dim NK cells upon activation. *J Immunol* 2007;178:4947–55.
19. Krause SW, Gastpar R, Andreesen R, et al. Treatment of colon and lung cancer patients with *ex vivo* heat shock protein 70-peptide-activated, autologous natural killer cells: a clinical phase I trial. *Clin Cancer Res* 2004;10:3699–707.
20. Specht HM, Ahrens N, Blankenstein C, et al. Heat shock protein 70 (Hsp70) peptide activated natural killer (NK) cells for the treatment of patients with non-small cell lung cancer (NSCLC) after radiochemotherapy (RCTx) – from preclinical studies to a clinical phase II trial. *Front Immunol* 2015;6:162.
21. Balermipas P, Rödel F, Krause M, et al. The PD-1/PD-L1 axis and human papilloma virus in patients with head and neck cancer after adjuvant chemoradiotherapy: a multicentre study of the German Cancer Consortium Radiation Oncology Group (DKTK-ROG). *Int J Cancer* 2017;141:594–603.
22. Linge A, Lohaus F, Lock S, et al. HPV status, cancer stem cell marker expression, hypoxia gene signatures and tumour volume identify good prognosis subgroups in patients with HNSCC after primary radiochemotherapy: a multicentre retrospective study of the German Cancer Consortium Radiation Oncology Group (DKTK-ROG). *Radiother Oncol* 2016;121:364–73.
23. Tinhofer I, Stenzinger A, Eder T, et al. Targeted next-generation sequencing identifies molecular subgroups in squamous cell carcinoma of the head and neck with distinct outcome after concurrent chemoradiation. *Ann Oncol* 2016;27:2262–8.
24. Linge A, Lock S, Gudziol V, et al. Low cancer stem cell marker expression and low hypoxia identify good prognosis subgroups in HPV(–) HNSCC after postoperative radiochemotherapy: a multicentre study of the DKTK-ROG. *Clinical Can Res* 2016;22:2639–49.
25. Balermipas P, Rodel F, Rodel C, et al. CD8+ tumour-infiltrating lymphocytes in relation to HPV status and clinical outcome in patients with head and neck cancer after postoperative chemoradiotherapy: a multicentre study of the German cancer consortium radiation oncology group (DKTK-ROG). *Int J Cancer* 2016;138:171–81.
26. Lohaus F, Linge A, Tinhofer I, et al. HPV16 DNA status is a strong prognosticator of locoregional control after postoperative radiochemotherapy of locally advanced oropharyngeal carcinoma: results from a multicentre explorative study of the German Cancer Consortium Radiation Oncology Group (DKTK-ROG). *Radiother Oncol* 2014;113:317–23.
27. Ferlay J, Soerjomataram I, Dikshit R, et al. Cancer incidence and mortality worldwide: sources, methods and major patterns in GLOBOCAN 2012. *Int J Cancer* 2015;136:E359–E86.
28. Chaturvedi AK, Engels EA, Pfeiffer RM, et al. Human papillomavirus and rising oropharyngeal cancer incidence in the United States. *JCO* 2011;29:4294–301.
29. Stein AP, Saha S, Yu M, et al. Prevalence of human papillomavirus in oropharyngeal squamous cell carcinoma in the United States across time. *Chem Res Toxicol* 2014;27:462–9.
30. Lai S, El-Naggar AK. Differential expression of key cell cycle genes (p16/cyclin D1/pRb) in head and neck squamous carcinomas. *Lab Invest* 1999;79:255–60.
31. Califano J, Ahrendt SA, Meiningner G, et al. Detection of telomerase activity in oral rinses from head and neck squamous cell carcinoma patients. *Cancer Res* 1996;56:5720–2.
32. Geisler SA, Olshan AF, Weissler MC, et al. p16 and p53 Protein expression as prognostic indicators of survival and disease recurrence from head and neck cancer. *Clin Can Res* 2002;8:3445–53.
33. Boyle JO, Hakim J, Koch W, et al. The incidence of p53 mutations increases with progression of head and neck cancer. *Cancer Res* 1993;53:4477–80.
34. Koch WM, Brennan JA, Zahurak M, et al. p53 mutation and locoregional treatment failure in head and neck squamous cell carcinoma. *J Natl Cancer Inst* 1996;88:1580–6.
35. Wittekindt C, Wagner S, Mayer CS, et al. Basics of tumor development and importance of human papilloma virus (HPV) for head and neck cancer. *GMS Curr Top Otorhinolaryngol Head Neck Surg* 2012;11:Doc09.
36. Wagner S, Wittekindt C, Reuschenbach M, et al. CD56-positive lymphocyte infiltration in relation to human papillomavirus association and prognostic significance in oropharyngeal squamous cell carcinoma. *Int J Cancer* 2016;138:2263–73.
37. Schemper M, Smith TL. A note on quantifying follow-up in studies of failure time. *Control Clin Trials* 1996;17:343–6.
38. McShane LM, Altman DG, Sauerbrei W, et al. Reporting recommendations for tumour MARKer prognostic studies (REMARK). *Br J Cancer* 2005;93:387–91.
39. Team RC. R: a language and environment for statistical computing. Vienna, Austria: Foundation for Statistical Computing, URL <https://www.R-project.org>, 2015.
40. Gross C, Schmidt-Wolf IG, Nagaraj S, et al. Heat shock protein 70-reactivity is associated with increased cell surface density of CD94/CD56 on primary natural killer cells. *Cell Stress Chaper* 2003;8:348–60.
41. Weidle UH, Maisel D, Klostermann S, et al. Intracellular proteins displayed on the surface of tumor cells as targets for therapeutic intervention with antibody-related agents. *Cancer Genomics Proteomics* 2011;8:49–63.
42. Stangl S, Gehrman M, Riegger J, et al. Targeting membrane heat-shock protein 70 (Hsp70) on tumors by cmHsp70.1 antibody. *Proc Natl Acad Sci USA* 2011;108:733–8.
43. Ciocca DR, Calderwood SK. Heat shock proteins in cancer: diagnostic, prognostic, predictive, and treatment implications. *Cell Stress Chaper* 2005;10:86–103.
44. Kleinjung T, Arndt O, Feldmann HJ, et al. Hsp70 membrane expression on head and neck cancer biopsy – a target for NK cells. *Int J Radiat Oncol Biol Phys* 2003;57:820–6.
45. Nylandsted J, Gyrd-Hansen M, Danielewicz A, et al. Heat shock protein 70 promotes cell survival by inhibiting lysosomal membrane permeabilization. *J Exp Med* 2004;200:425–35.
46. Ang KK, Harris J, Wheeler R, et al. Human papillomavirus and survival of patients with oropharyngeal cancer. *N Engl J Med* 2010;363:24–35.
47. Mandal R, Şenbabaoglu Y, Desrichard A, et al. The head and neck cancer immune landscape and its immunotherapeutic implications. *JCI Insight* 2016;1:e89829.
48. Rietbergen MM, Martens-de Kemp SR, Bloemena E, et al. Cancer stem cell enrichment marker CD98: a prognostic factor for survival in patients with human papillomavirus-positive oropharyngeal cancer. *Eur J Cancer* 2014;50:765–73.
49. Zhang Y, Xiong Y, Yarbrough WG. ARF promotes MDM2 degradation and stabilizes p53: ARF-INK4a locus deletion impairs both the Rb and p53 tumor suppression pathways. *Cell* 1998;92:725–34.
50. Agrawal N, Frederick MJ, Pickering CR, et al. Exome sequencing of head and neck squamous

- cell carcinoma reveals inactivating mutations in NOTCH1. *Science* 2011;333:1154–7.
51. Botzler C, Schmidt J, Luz A, et al. Differential Hsp70 plasma membrane expression on primary human tumors and metastases in mice with severe combined immunodeficiency. *Int J Cancer* 1998;77:942–8.
52. Horvath I, Multhoff G, Sonnleitner A, et al. Membrane-associated stress proteins: more than simply chaperones. *Biochim Biophys Acta* 2008; 1778:1653–64.
53. Breuninger S, Erl J, Knape C, et al. Quantitative analysis of liposomal heat shock protein 70 (Hsp70) in the blood of tumor patients using a novel LipHsp70 ELISA. *Clin Cell Immunol* 2014; 5:2–10.
54. Gehrman M, Specht HM, Bayer C, et al. Hsp70 – a biomarker for tumor detection and monitoring of outcome of radiation therapy in patients with squamous cell carcinoma of the head and neck. *Radiat Oncol* 2014;9: 131–40.
55. Thorsteinsdottir J, Stangl S, Fu P, et al. Overexpression of cytosolic, plasma membrane bound and extracellular Hsp70 in primary glioblastomas. *J Neurooncol* 2017;135: 443–52.